Acta Cryst (1996). D**52**, 543–550

E144S Active-Site Mutant of the *Bacillus cereus* Thermolysin-Like Neutral Protease at 2.8 Å Resolution

S. A. LITSTER,[a] D. R. WETMORE,[b]† R. S. ROCHE[b] AND P. W. CODDING[a]*

[a]*Departments of Chemistry and of Pharmacology and Therapeutics, and* [b]*Department of Biological Sciences, University of Calgary, Calgary, Alberta, Canada. E-mail: pcodding@acs.ucalgary.ca*

(*Received 25 July 1995; accepted 11 December 1995*)

Abstract

The X-ray crystal structure of the *Bacillus cereus* neutral protease (CNP) active-site mutant E144S, in which the putative general base proposed for the thermolysin-like zinc neutral proteases, Glu144, has been replaced by serine, has been determined to a resolution of 2.8 Å. This represents the first crystal structure of an active-site mutant of a zinc neutral protease. The E144S mutant was crystallized in the hexagonal space group, $P6_522$, with unit-cell dimensions $a = b = 76.57$, $c = 201.91$ Å. Although the ligands involved in zinc coordination in the active site are identical to those found in the wild-type protein, the mutation results in a modified environment around the zinc ion; particularly with respect to the water molecules. While the structure of the mutant is similar to that of wild type, its protease activity is reduced to 0.16% that of the wild-type CNP and the protein is virtually resistant to autolysis in the presence of calcium. The lowered protease activity of the mutant is consistent with the role proposed for Glu144 as the general base in the catalysis of thermolysin-like neutral proteases [Matthews (1988). *Acc. Chem. Res.* **21**, 333–340]. We suggest that the residual activity of the E144S mutant arises from a water molecule, which is found within hydrogen-bonding distance of Ser144, acting as a general base in the catalytic function of the mutant.

1. Introduction

Bacillus cereus neutral protease (CNP) is a thermolysin-like zinc metalloendopeptidase (molecular weight 34 kDa) which hydrolyses polypeptide chains at the amino side of hydrophobic and aromatic residues (Feder, Keay, Garrett, Cirulis, Moseley & Wildi, 1971; Sidler, Kumpf, Peterhans & Zuber, 1986). The thermolysin-like neutral proteases (TNP's; Wetmore, Wong & Roche, 1992) are now recognized as one subgroup of the 'zincin' super-family of proteases (Bode, Gomis-Rüth & Stocker, 1993; reviewed by Blundell, 1994; Stocker, Grams, Baumann, Reinemer, Gomis-Rüth, McKay & Bode, 1995) members of which, like the matrix metalloproteinases (MMP's), are associated with degenerative diseases such as rheumatoid arthritis, osteoarthritis and tumor metastasis. In the thermolysin-like subgroup of the zincin super family, the zinc-binding ligands and the catalytically important general-base are included in the consensus sequence HEXXH(+20)NEXSD. The zinc is tetrahedrally coordinated by the two His residues and the Glu residue 20 amino acids downstream from the N-terminal of the consensus sequence. A water molecule provides the fourth ligand. The Glu residue proximal to the first His is believed to be the catalytic general-base. CNP shares 73% sequence identity with thermolysin (Holland *et al.*, 1992) and adopts a similar two-domain fold (Pauptit *et al.*, 1988; Stark, Pauptit, Wilson & Jansonius, 1992): the N-terminal domain mainly β-pleated sheet and the C-terminal domain mainly α-helical, with the zinc-containing active-site cleft between the two domains. In addition to the zinc ion, TNP's bind up to four calcium ions which modulate the kinetics of autolysis and thermal unfolding of the molecule (Roche & Voordouw, 1978).

The catalytic mechanism proposed for the TNP's is based on crystallographic studies of protease–inhibitor complexes of thermolysin (Matthews, 1988). It is proposed that the binding of substrate displaces the ligating water molecule toward Glu143 (numbering for thermolysin), which plays a key role by acting as a general base. The activated water molecule then attacks the carbonyl C atom of the scissile bond, which is also polarized by the zinc. Catalysis proceeds *via* a tetrahedral intermediate. The carbonyl O atom of the scissile bond forms a hydrogen bond with His231 in the transition intermediate. In CNP, the corresponding active-site residues are His143, His147 and Glu167, which provide the zinc ligands, and Glu144 which is in the homologous position to the putative general base Glu143 of thermolysin. Based on these results, and those of mutagenesis studies of neutral protease A (Toma *et al.*, 1989), which showed that the mutants E143S and E143W (numbering for neutral protease A) have no catalytic activity, the mutation E144S was designed.

† Present address: Physical Sciences Division, DuPont Merck Pharmaceutical Co., Experimental Station E328/B48B, Wilmington, DE 19880-0328, USA.

Here we describe the crystallization, crystallographic analysis and refinement of the structure of the E144S mutant at 2.8 Å resolution. The structure is compared with wild-type CNP and the differences are discussed in the light of the observed differences in the proteolytic activity of the two proteins.

2. Materials and methods

2.1. *Crystallization*

The mutant enzyme was isolated, purified and assayed with the general protease substrate azocasein, as previously described for the wild-type enzyme (Wetmore, Wong & Roche, 1992, 1994). The storage buffer for the protein [50 m*M* Tris-(hydroxymethyl)-aminomethane, 10 m*M* NaCl, 10 m*M* $CaCl_2$, (pH 6)] was exchanged by dialysis against 50 m*M* potassium succinate containing 10 m*M* $CaCl_2$ at pH 6. Concentration to 12 mg ml^{-1} was achieved by dialysis against a buffered 18% polyethylene glycol (M_r 20 000) solution.

Crystallization was carried out using the hanging-drop vapour-diffusion method (Davies & Segal, 1971) against a reservoir solution containing 16%(*w*/*v*) polyethylene glycol (PEG 6000) in 50 m*M* potassium succinate buffer (pH 6) and 10 m*M* $CaCl_2$. The crystal size and morphology were found to be dependent on the volume ratio of reservoir to protein solution making up the hanging drop. Drops initially containing 8 µl reservoir solution and 8 µl protein solution produced hexagonal bipyramidal prisms with maximum dimensions of 0.15 mm. This is the same crystal form as reported for wild-type CNP (Pauptit *et al.*, 1988). However, an initial drop ratio of 4 µl reservoir solution to 8 µl protein solution produced hexagonal bipyramidal needles with maximum dimensions of 0.7 × 0.3 × 0.3 mm. Crystals of this needle morphology suitable for X-ray analysis grew within 16 d: 2 d at 273 K followed by 14 d at 279 K. The crystals belong to the hexagonal space group $P6_522$ and have unit-cell dimensions $a = b = 76.57$, $c = 201.92$ Å. These values are comparable to those obtained for the prism morphology exhibited by wild-type CNP which also crystallizes in the hexagonal space group, $P6_522_1$ and has unit-cell dimensions $a = b = 76.5$, $c = 201.0$ Å. There is one 34 kDa monomeric molecule per asymmetric unit and 12 molecules per unit cell of volume 1.03×10^6 Å^3. The solvent content is 51%.

2.2. *Data collection and processing*

The diffraction data were recorded at 287 K on the FAST area detector (at the Department of Biochemistry, University of Saskatoon) with copper radiation and a rotating-anode generator at 40 kV and 95 mA. A single crystal 0.50 × 0.25 × 0.25 mm was mounted in a glass capillary along with mother liquor and the ends of the capillary sealed with wax. The crystallographic *c* axis was oriented at 30° to the rotation axis. The detector was placed 14.5 cm away from the crystal in order to resolve the reflections in the direction of the *c* axis, and data were collected to 2.8 Å resolution. The data were processed using the on-line *MADNES* program and the *CCP*4 suite of programs (Collaborative Computational Project, Number 4, 1994). A total of 47 398 reflections were measured to 2.8 Å resolution. The final R_{sym} value was 7.7% for 8508 unique reflections; which made up 89% of the unique data. The final shell of data, 3.0–2.8 Å, was 87.5% complete.

2.3. *Structure determination and refinement*

Since the differences in the unit-cell dimensions of the E144S mutant and wild-type CNP were less than 0.5% the 2 Å model of wild-type CNP (Stark *et al.*, 1992) was used as the starting model. To prepare an initial model, the coordinates of the wild-type structure were edited to remove the water molecules and Glu144 was changed to serine using the Biopolymer module of the *InsightII*™ program (Biosym Technologies, 1993).

In the first step of refinement the molecule, consisting of 2700 non-H atoms in 317 amino acids, was subjected to rigid-body least-squares refinement using the *X-PLOR* program (Brünger, 1992). The refinement was performed on 5990 reflections in the resolution range 10–3.0 Å. The crystallographic *R* value was initially 0.45 and was lowered in 40 successive cycles to 0.31. At this point in the refinement, the resolution range was extended to 2.8 Å. Constraints were used to fix the bond lengths and angles to 'ideal' values throughout the refinement process, whilst the constraints fixing the atomic positions were removed stepwise over 50 cycles of Powell minimization in the order: side-chain atoms, backbone atoms, Cα atoms. Refinement of the atomic positions was followed by 40 cycles of individual temperature-factor refinement resulting in an *R* value of 0.21. A $(2F_o - F_c)$ map and a series of annealed $(F_o - F_c)$ maps (Hodel, Kim & Brünger, 1992), with residue 144 omitted, were calculated and examined. A number of minor adjustments were made to side chains, and water molecules were included. Iterative refinement using a combination of simulated annealing (temperature range 3000–300 K, temperature step 25 K, time step 0.5 fs), Powell minimization and manipulation of the molecule resulted in a final *R* value of 0.178. Water molecules were included in the model if they displayed electron density in a $2F_o - F_c$ map, contoured at 1.0σ above the mean, and their thermal parameters refined to a value below 70 Å^2. The final model included 2391 protein atoms and 100 solvent molecules.*

* Atomic coordinates and structure factors have been deposited with the Protein Data Bank, Brookhaven National Laboratory (Reference: 1ESP, R1ESPSF). Free copies may be obtained through The Managing Editor, International Union of Crystallography, 5 Abbey Square, Chester CH1 2HU, England (Reference: GR0466).

3. Results

The electron density in the active site of the mutant CNP is shown in Fig. 1(*a*). Fig. 1(*b*) shows the density due to the active-site water molecules.

The mean coordinate error of the final model is estimated from the variation of the R factor with resolution (Luzzati, 1952), to lie between 0.25 and 0.30 Å. Most of the structure is well defined with the higher B values associated with residues in surface loops (residues 23–32, 125–133, 197–203, 217–228, 250–254 and 282–287). The final model conforms to accepted stereochemistry with standard deviations from ideal bond lengths and angles of 0.016 Å and 1.157°, respectively. Examination of the Ramachandran plot (Fig. 2) shows that all non-glycine residues with the exception of residues Asn61, Ser93, His106, Ser153 and Asn160, lie in the 'allowed' regions. The positions of these five residues were confirmed by examining annealed $(F_o - F_c)$ maps generated with the respective residues omitted (Fig. 3).

Discussion

Previous studies of the thermolysin-like neutral proteases have shown that a narrowing of the active-site cleft occurs when an inhibitor binds to the active site (Holland *et al.*, 1992). The movement of the two domains has been described as a 'hinge-bending' motion, in which the N-terminal and C-terminal domains move about a central point, known as the 'flexible hinge region', identified to lie between residues 132 and 136 (thermolysin numbering). The degree of 'hinge bending' can be calculated by superimposing the N-terminal domains of the two structures being compared, and then determining the angle of rotation required to bring the C-terminal domain of one protein into register with the other (Holland *et al.*, 1992). We achieved this by first calculating a 'best fit' vector, representing the principal moment of inertia of a set of atoms with a uniform mass of 1, for the backbone atoms of E144S and CNP. The hinge-bending angle was then calculated by summing the angles between the two vectors as the N-terminal and C-terminal domains were independently superimposed. The angle between the two vectors on superimposing the N-terminal domains (residues 1–130) was found to be 1.68°, and the corresponding angle on superimposing the C-terminal domains, 0.40°, giving a total hinge-bending angle, representing a contraction, of 2.08°, on going from CNP to E144S. To test the technique we performed the same calculation using CNP and thermolysin. We obtained a hinge-bending angle of 5.8°, which compares well to the value of 6° reported by Holland *et al.* (1992).

Using data obtained from an inter-domain difference Cα distance plot, we calculated that the average contraction on going from CNP to E144S was 0.5 Å. The observed domain contraction (Fig. 4) on going from CNP to E144S may be rationalized in terms of the changes in the steric and electrostatic interactions when Glu144 is replaced by the serine residue. Residue 144 occupies a highly influential, central position in the active site of the protein. It is located in the C-terminal domain close to the flexible hinge region (residues 132–136), and lies midway between the zinc ion and residues 114–122 of the N-terminal domain. Replacing a Glu by a Ser residue results in a reduction of the steric interactions between the N-terminal and C-terminal domains.

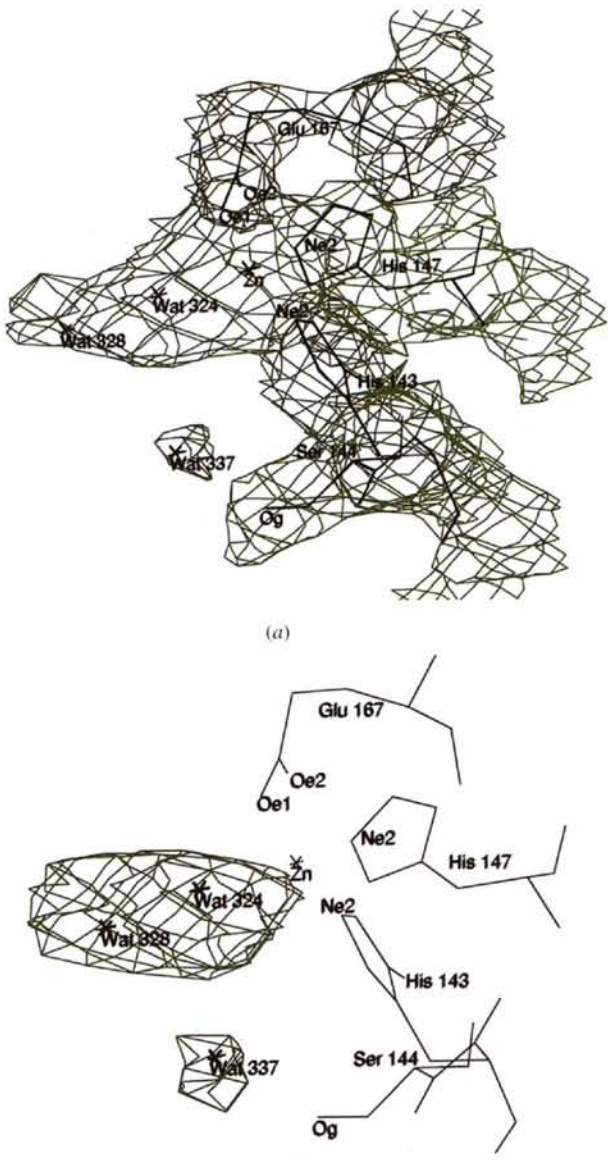

Fig. 1. Active site of the refined structure of the E144S mutant superimposed on: (*a*) the $(2F_o - F_c)$ electron-density map of the active-site residues. The map is contoured at the 1σ level. (*b*) $(F_o - F_c)$ map showing the positions of the water molecules in the active site. The map is contoured at 1.2σ above the mean density. The program *Xtalview* (McRee, 1992) was used to plot the electron density.

However, this is a short-range steric effect and it is difficult to assess its consequences on the entire structure. A more probable explanation for the domain contraction can be given in terms of the longer ranging electrostatic interactions. The global effect of replacing a glutamic acid by a serine is to reduce the overall negative charge on the protein by 1. The local effect would be a reduction in the electrostatic repulsive forces between the negatively charged Glu144 residue and the surrounding acidic residues; a number of which are found in two large α-helices which dominate the central core of the molecule. The α-helix 138–151 (acidic residues, 139 and 151) spans the width of the molecule, and lies directly between the N-terminal and C-terminal domains. The larger α-helix, residues 161—181 (acidic residues, 161, 167, 171, 178 and 181) runs diagonally across the C-terminal and terminates at a point close to the N-terminal domain. A collapse of these α-helices toward the region of the mutation would likely cause the observed domain contraction and a hinge-bending motion.

4.1. *Calcium ion binding sites*

The molecule binds four calcium ions (Fig. 4). Calcium ions 1, 2 and 4 are located in the C-terminal domain, and calcium ion 3 binds in the N-terminal domain. All four ions are found to have coordination numbers in the range five to seven as observed in CNP and TLN. With the exception of two water ligands, the structure and coordination of the calcium-binding sites in E144S are essentially the same as those found in the structure of CNP. At this resolution there are some statistically significant differences in ligand calcium distances. However, higher resolution data is needed to assess their importance.

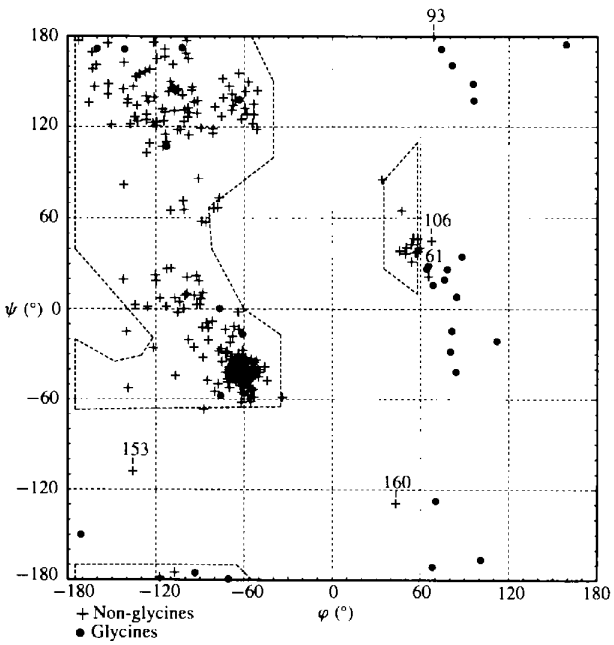

Fig. 2. Ramachandran plot. Backbone torsion angles (φ, ψ) of E144S. Non-glycine residues are marked with + and glycine residues are marked with ●. The five non-glycine residues that lie outside of the allowed regions are labeled by sequence number.

4.1.1. *S(1)/S(2) site.* Calcium ions 1 and 2 bind to a double binding site at a distance of 3.85 Å apart. They share the coordination of three carboxyl groups: Glu178, Asp186 and Glu191 which act as bridging ligands. In addition, Ca1, the inner of the two ions, is ligated by the Oδ1 of Asp139 and the backbone O atom of Glu188. The coordination of Ca1 is completed by one solvent molecule, Wat374, which is also bound to the protein through the formation of a hydrogen bond with the Oε2 of Glu178; r(O···O) = 2.71 Å. The outer calcium ion is located at the entrance to the double binding site, close to the surface of the molecule and, in addition to the bidentate ligands it shares with Ca1, it is ligated by Wat380. A ligating water molecule, Wat357 found in the CNP structure is not found in E144S (Table 1).

The position and relative flexibility of the two sites are reflected by differences in the thermal parameters, values of 12.53 and 21.13 Å^2 are calculated for Ca1 and Ca2, respectively, and average thermal parameters of 19.77 and 25.88 Å^2 are found for the ligating residues in sites S(1) and S(2), respectively.

4.1.2. *S(3) site.* A surface loop, residues 58 to 62, provides three ligands to the Ca3 ion, the remaining three ligands are supplied by the solvent. The thermal parameter of the ion is 20.85 Å^2, and, as with the S(1)–S(2) sites, the average temperature factor of the ligating residues is approximately 7 Å^2 higher. The thermal parameters of the ligating water molecules, Wat348, Wat390 and Wat391, are 18.08, 41.30 and 30.20 Å^2, respectively. These thermal parameters are consistent with the observation that both Wat348 and Wat391 form hydrogen bonds with the carboxyl side chains of Asp60, r(391O···60Oδ1) = 2.82 Å and Asp68, r(348O··· 68Oδ2) = 2.88 Å, whereas Wat390 does not.

4.1.3. *S(4) site.* The S(4) site is located in a surface loop, residues 197 to 203. The average thermal parameters for the ligating atoms (Table 1) are higher than those for the other calcium-binding sites. The temperature factor of the Ca4 ion is 27.40 Å^2 and the average temperature factor of the ligands is 31.42 Å^2. The average thermal parameter for the backbone atoms of the loop, 33.2 Å^2, suggests that this is a very flexible region.

4.2. *Active site*

A least-squares superposition, using the *InsightII*™ superposition algorithm (Biosym Technologies, 1993), of the zinc ions and the Cα atoms of residues 142–148, 165–171, of E144S and CNP produces a root-mean-

square difference of just 0.15 Å indicating that the overall geometry of the active site has not significantly changed. However, inspection of the two sites in E144S and CNP (Fig. 5) reveals differences in the zinc coordination and the arrangement of the ordered water molecules in the active-site cleft. The active site of E144S contains two extra water molecules compared with CNP. One, Wat328, is positioned at the entrance to the active site and is hydrogen bonded to the water molecule ligated to zinc, Wat324, $r(324\,O\cdots328O) = 2.91$ Å. The other water molecule, Wat337, is hydrogen bonded to the Oγ atom of Ser144, $r(337\,O\cdots144O\gamma) = 3.37$ Å and occupies the space vacated by the carboxyl group of Glu144 upon mutation to serine.

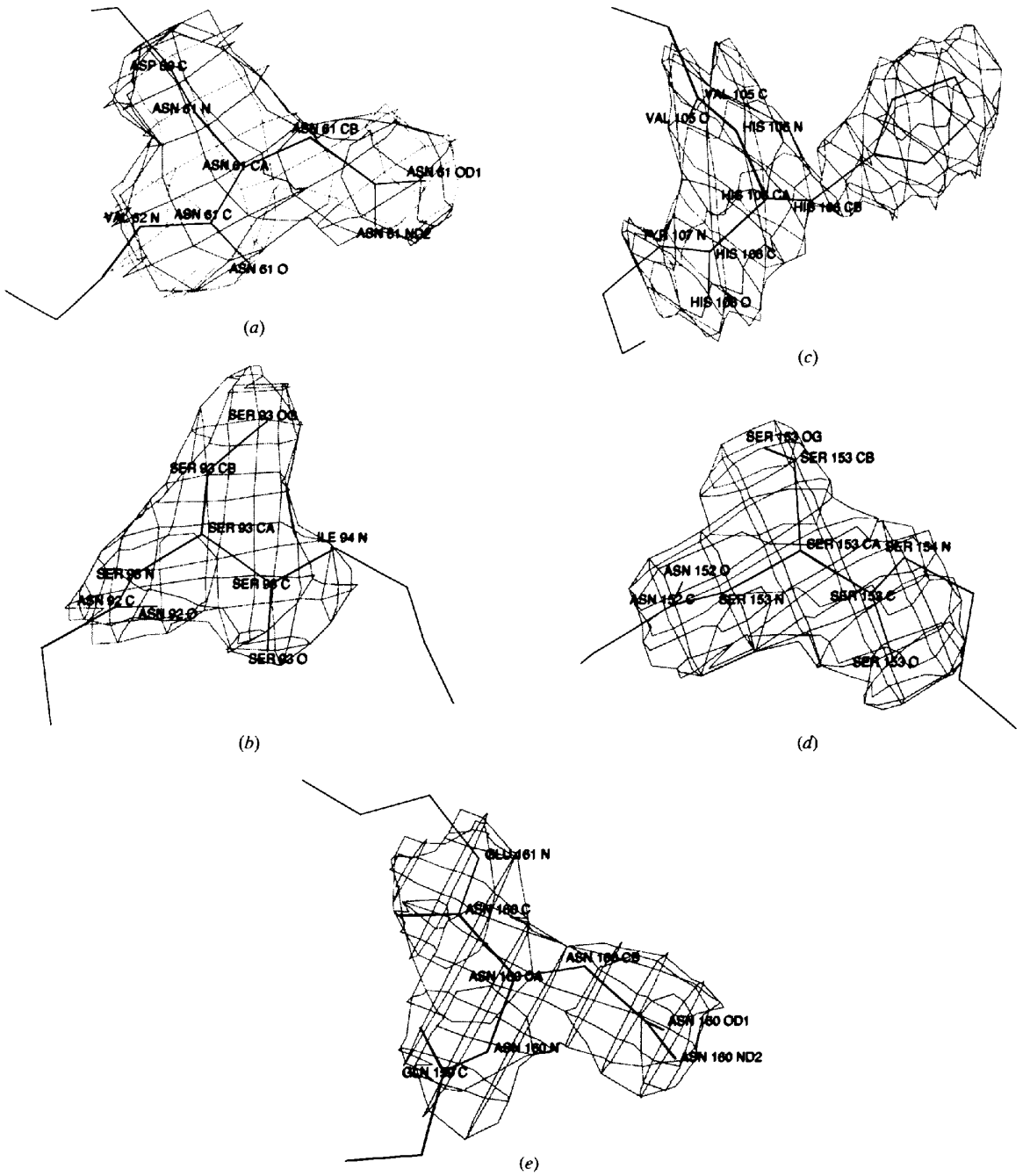

Fig. 3. Refined structure superimposed on the $(F_o - F_c)$ map with the following residue omitted: (*a*) Asn61, (*b*) Ser93, (*c*) His106, (*d*) Ser153, (*e*) Asn160.

Table 1. *Metal-ion coordination*

Metal Ion	Residue/atom	Ion–ligand distances (Å) CNP	E144S
Ca1	Asp139 Oδ1	2.44	2.68
	Glu178 Oε2	2.56	2.27
	Asp186 Oδ1	2.49	2.53
	Glu188 O	2.29	2.10
	Glu191 Oε1	2.44	2.48
	Glu191 Oε2	2.66	2.50
	Wat374 O	2.45	2.42
Ca2	Glu178 Oε1	2.49	2.29
	Asn184 O	2.49	2.35
	Asp186 Oδ2	2.40	2.26
	Glu191 Oε2	2.41	2.16
	Wat389 O	2.20	2.34
	Wat357 O	2.44	*
Ca3	Asp58 Oδ1	2.44	2.41
	Asp58 Oδ2	2.60	2.36
	Asp60 Oδ1	2.35	2.69
	Val62 O	2.23	2.58
	Wat348 O	2.53	2.19
	Wat390 O	2.72	2.36
	Wat391 O	2.31	2.21
Ca4	Tyr194 O	2.26	2.43
	Thr195 O	2.37	2.20
	Thr195 Oγ1	2.58	2.54
	Lys198 O	2.36	2.28
	Asp201 Oδ1	2.41	2.30
	Wat392 O	2.13	2.37
	Wat380 O	2.59	*
Zn	His143 Nε2	2.17	2.11
	His147 Nε2	2.05	1.97
	Glu167 Oε1	2.48	2.95
	Glu167 Oε2	2.10	1.95
	Wat324 O	1.96	2.19

* These water molecules were not observed in the E144S structure.

4.3. *Zinc coordination*

As in CNP, the zinc ion in E144S adopts a distorted tetrahedral geometry. In the mutant structure the positions of the zinc ion, the Nε2 atoms of His143 and His147 remain approximately the same as in the wild-type structure (see Fig. 5). There are differences in the Zn to ligand atom distances (Table 1); however, higher resolution data is needed to assess their importance. In the E144S structure, two ligands, the Oε1 of Glu167 and Wat324, move away from the zinc ion by 0.47 and 0.23 Å, respectively. The shift in Glu167 takes the Oε1 atom out of bonding range of the Zn. The changes in the zinc coordination are further characterized by the angles defined in Table 2. The largest changes are associated with the movement of Glu167 and Wat324. There are also changes in the side-chain χ angles of His143 and Glu167. In the case of His143, χ_2 increases from 100.3 to 147.9°. In Glu167, χ_3 decreases from 139.9 to 113.8°. The other χ values for both residues show no statistically significant changes.

4.4. *Enzyme activity of E144S*

A comparison of the activity of E144S and CNP toward peptide substrates showed that the E144S mutant has only 0.16% of the wild-type peptidase activity toward the general peptide substrate, azocasein (Wetmore, 1993). This confirms the suggestion (Matthews, 1988) that the active-site glutamic acid residue plays a key role in the mechanism of peptide hydrolysis by neutral proteases, acting as a general base and raises the question: why does the E144S mutant show residual peptidase activity?

The residual peptidase activity is low and requires a higher free energy of activation; Wetmore (1993) found that the free energy of activation for the hydrolysis of azocasein is 3.8 kcal mol^{-1} higher for the E144S mutant than for CNP. The X-ray crystal structure of the E144S mutant suggests that Wat337, which is hydrogen bonded to the Oγ atom of Ser144 (see Fig. 5), may act as the general base in lieu of Glu144. The difference in peptidase activity between CNP and E144S may be

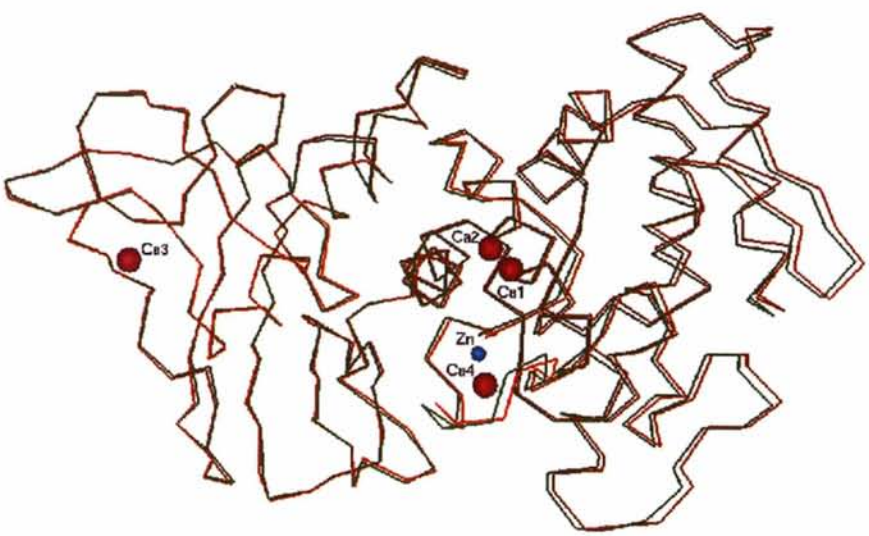

Fig. 4. Superposition of the N-terminal Cα atoms of E144S (green) and CNP (red) using least squares (Biosym Technologies, 1993). The superposition resulted in a root-mean-square deviation, calculated over all Cα atoms, of 0.38 Å.

Table 2. *Zinc coordination angles*

Angle	CNP (°)	E144S (°)	Difference (°)
His143 (Nε2—Zn—Nε2) His147	105	112	7
His143 (Nε2—Zn—Oε2) Glu167	120	97	−23
His143 (Nε2—Zn—O) Wat324	105	109	4
His147 (Nε2—Zn—Oε2) Glu167	107	109	2
His147 (Nε2—Zn—O) Wat324	95	129	34
Glu167 (Cδ—Zn—O) Wat324	120	96	−24

due to the differences in the ability of Glu144 and an activated water molecule (Wat337) to act as a base. Based on pK_a values, a glutamic acid residue, pK_a 4.20, would be a more effective general base, by at least three orders of magnitude, than the activated water molecule, assuming that the pK_a of an activated water molecule lies between the minimum value calculated for a zinc-activated water molecule, pK_a 7.0, and the value in bulk water, pK_a15.7 (Christianson, 1991). Water molecules act as the general base in the catalytic mechanisms of staphylococcal nuclease, carbonic anhydrase I and *ras* p21 (Åqvist & Warshel, 1990, 1992; Schweins, Langen & Warshel, 1994). The calculated difference in free energy between a water molecule as general base and the carboxylate general base in staphylococcal nuclease is 5 kcal mol^{-1}; a value similar in magnitude to the experimental difference in the free energy of activation determined for E144S compared to CNP.

The proposed mechanism would proceed similarly to that proposed for thermolysin (Matthews, 1988) with the exception that the attacking water molecule, Wat324, is further activated by interactions with the hydrogen-bonded water molecule, Wat337. In this mechanism, the incoming peptide would displace the zinc-bound water molecule, Wat324, toward the hydrogen-bonded water molecule Wat337 followed by nucleophilic attack by Wat324 on the carbonyl group of the substrate. The transfer of a proton to the leaving N atom of the substrate could be accomplished *via* a shuttle mechanism involving the ordered water molecules in the active site.

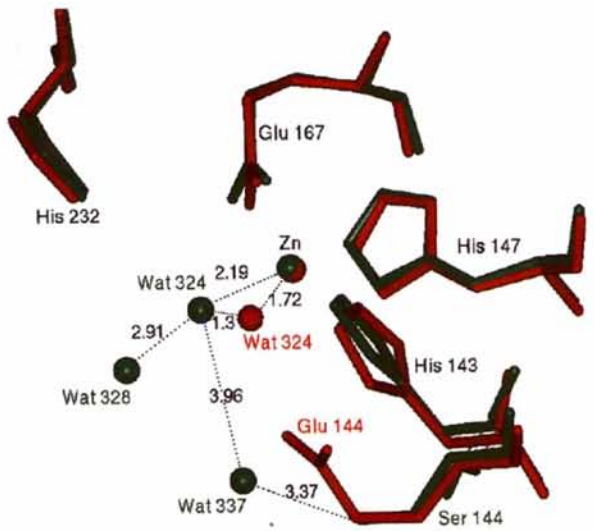

Fig. 5. Comparison of the active sites in the E144S mutant (green), and the native protein, CNP (red). The zinc ions and the Cα atoms of residues 142–148 and 165–171, were superimposed using least squares (Biosym Technologies, 1993). In the E144S structure there are two extra water molecules, Wat328 and Wat337, and the position of the zinc ligand, Wat324, is shifted with respect to residues 144 and 232. In addition, the orientation of the side chains of residues His143 and Glu167 are shifted in the E144S structure.

5. Concluding remarks

This 2.8 Å resolution study of the E144S mutant has given us insight into how and why the single point mutation, E144S, renders the CNP molecule almost totally inactive as a peptidase even though the two structures are nearly identical. This provides further evidence for the role of Glu144 as the general base in the peptidase activity of the wild-type protein, CNP. In addition, the structure highlights the importance of the water molecule in the mechanism of catalysis in the neutral proteases.

We are growing both the hexagonal bipyramid needle and hexagonal bipyramidel prism forms of E144S to determine whether the domain contraction observed in the inactive mutant is a result of differences in electrostatic/steric interactions or morphological forms. We are also carrying out soaking experiments with a variety of peptide and ester substrates on the crystals to examine what effects a bound substrate would have on overall structure of the protein, and more importantly, what interactions are present between the enzyme and the substrate in the active site. The ultimate goal is to gain a deeper understanding into the mechanisms and structure–function relationships of the zinc metallo-proteases.

The authors thank Dr L. T. J. Delbaere and M. Vandonselaar at the University of Saskatoon, for providing access to the FAST area-detector data-collection facility and for help processing the data. Financial support from the Alberta Heritage Foundation for Medical Research (fellowship to SAL, scholarship to DRW), the Medical Research Council (grant to PWC), the National Science and Engineering Research Council (grant to RSR, scholarship to DRW) is gratefully acknowledged. The authors also thank the University of Calgary, for generous computer support.

References

Åqvist, J. & Warshel, A. (1990). *J. Am. Chem. Soc.* **112**, 2860–2868.
Åqvist, J. & Warshel, A. (1992). *J. Mol. Biol.* **224**, 7–14.
Biosym Technologies (1993). *InsightII User Guide, Version 2.2.0,* Biosym Technologies, San Diego, CA, USA.
Blundell, T. L. (1994). *Nature Struct. Biol.* **1**(2), 73–75.

Bode, W., Gomis-Rüth, F. X. & Stocker, W. (1993). *FEBS Lett.* **331**(1–2), 134–140.

Brünger, A. T. (1992). *X-PLOR Version 3.0 Manual,* Yale University, New Haven, CT, USA.

Christianson, W. (1991). *Adv. Protein Chem.* **42**, 301–302.

Collaborative Computational Project, Number 4 (1994). *Acta Cryst.* D**50**, 760–763.

Davies, D. R. & Segal, D. M. (1971). *Methods Enzymol.* **22**, 266–269.

Feder, J., Keay, L., Garrett, L. R., Cirulis, N., Mosely, M. H. & Wildi, B. S. (1971). *Biochim. Biophys. Acta,* **251**, 74–78.

Hodel, A. H., Kim, S. H. & Brünger, A. T. (1992). *Acta Cryst.* A**48**, 851–858.

Holland, D. R., Tronrud, D. E., Pley, H. W., Flaherty, K. M., Stark, W., Jansonius, J. N., McKay, D. B., Matthews, B. W. (1992). *Biochemistry,* **31**, 11310–11316.

Luzzati, V. (1952). *Acta Cryst.* **5**, 802–810.

McRee, D. E. (1992). *J. Mol. Graph.* **10**, 44–46.

Matthews, B. W. (1988). *Acc. Chem. Res.* **21**, 333–340.

Pauptit, R. A., Karlsson, R., Picot, D., Jenkins, J. A., Nicklaus-Reimer, A. S. & Jansonius, J. N. (1988). *J. Mol. Biol.* **199**, 525–537.

Roche, R. S. & Voordouw (1978). *Crit. Rev. Biochem.* **5**, 1–25.

Schweins, T., Langen, R. & Warshel, A. (1994). *Nature Struct. Biol.* **1**(7), 476–484.

Sidler, W., Kumpf, B., Peterhans, B. & Zuber, H. (1986). *Appl. Microbiol. Biotechnol.* **25**, 18–24.

Stark, W., Pauptit, R. A., Wilson, K. S. & Jansonius, N. J. (1992) *Eur. J. Biochem.* **207**, 781–791.

Stocker, W., Grams, F., Baumann, U., Reinemer, P., Gomis-Rüth, F.-X., McKay, D. B. & Bode, W. (1995). *Protein Sci.* **4**, 823–840.

Toma, S. Campagnoli, S., De Gregoris, S., Gianna, R., Margarit, I., Zamai, M. & Grandi, G. (1989). *Protein Eng.* **2**, 359–364.

Wetmore, D. R. (1993). PhD thesis. University of Calgary, Calgary, Alberta, Canada.

Wetmore, D. R., Wong, S.-L. & Roche, R. S. (1992). *Mol. Microbiol.* **6**(12), 1593–1604.

Wetmore, D. R., Wong, S.-L. & Roche, R. S. (1994). *Mol. Microbiol.* **12**(5), 747–759.